

Opto-Mechanical Design and Error Analysis of Digital System Measuring Refractive Index

Cao Miao¹, Wang Xiao¹, Yan Juncen² and Shen Yingchun³

¹*Changchun University of Science and Technology, Jilin Changchun,
130022, China*

²*Changchun University Of Technology, Jilin Changchun, 130012, China*

³*Changchun Tiannuo precision measurement and Control Technology Co Ltd,
Jilin Changchun, 1300222, China
79816540@qq.com*

Abstract

This paper proposes a new general design scheme about the digital system measuring refractive index. It is based on CCD machine vision alignment technique. This system is mainly composed of auto-collimator, transmission mechanism, locking and trimming mechanism, and incremental encoder goniometer institution. First of all, to meet the demand in a wide spectrum of various aberrations, the auto-collimated optical system is designed, which achieve a good image quality. Secondly, the spiral trimming mechanism is designed, and in accordance with the micros-tress assembling method the locking mechanism is achieved. The out shaft of photoelectric encoder can move slowly and steadily, and ensure its position more precise adjustment. Finally, the detection error is analyzed based on the principle of correction formulas to consider the influence of air refractive index. The experimental results show that the system can measure the refractive index of transparent material such as glass, and the accuracy of refractive index detection is up to $\pm 3 \times 10^{-6}$.

Keywords: *Refractive index, Optical and mechanical structure, CCD vision alignment, error analysis*

1. Introduction

The refractive index of optical glass is an important basis for optical system design in optoelectronic devices. Its accuracy is directly related to the design quality and image quality of the optical system. Thus, in the manufacture of optical glass and detection device, the refractive index of the optical glass can affect the quality of optical instrument to a great extent [1]. Therefore, lots of optical glass manufacturers need high-precision measurement on refractive index, to serve the testing session of optical glass production line and to obtain high-quality optical glass. Through comprehensive consideration of factors that affect the measurement of the refractive index of optical glass, this paper develops a refractive index measurement system, whose measurement accuracy is $\pm 3 \times 10^{-6}$.

At present, the maximum refractive index measurement accuracy of only $\pm 3 \times 10^{-5}$ [3]. In this paper, the mechanical structure of the traditional system measuring refractive index is improved. The original mechanical goniometer is replaced by incremental photoelectric encoder to measure the angle of refraction. Its original angle measuring accuracy improves from original $\pm 3''$ to $\pm 1''$. Visual alignment in traditional instruments is improved with machine vision alignment based on CCD imaging technology. Taking the influence of the refractive index of air into account, the principle of correction formula is given, and the errors of the system is also analyzed on this basis.

2. Composition of Digital System Measuring Refractive Index

The structure of digital system measuring refractive index is shown in Figure 1. This system is mainly composed of auto-collimator, condenser, transmission mechanism, prism, locking and trimming mechanism, incremental encoder goniometer institution, CCD camera, and the part to be measured.

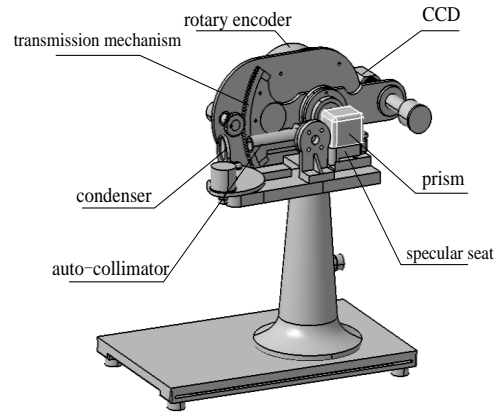


Figure 1. Digital System Measuring Refractive Index

To improve the measurement accuracy of digital system measuring refractive index, and to meet the requirements of small size, convenience and so on, the key technical parameters of opto-mechanical system is determined, as shown in Table 1.

Table 1. The Key Technical Parameters of Opto-Mechanical System

| design project | parameters |
|--|---------------|
| focal length of auto-collimator/ <i>mm</i> | 180 <i>mm</i> |
| aperture/ <i>mm</i> | 18 <i>mm</i> |
| field/ ° | 5° |
| standard deviation of deflection angle/ " | ≤4" |
| CCD swing range/ ° | ±30° |

The digital system measures refractive index with photoelectric rotary encoder to measure the deflection angle of refracted light, In order to achieve precise to obtain the image of light refraction with CCD image sensor. According to the functional requirements of the system, auto-collimator, transmission mechanism, locking and trimming mechanism and incremental encoder goniometer clamping institution are designed. The appropriate aperture and focal length of auto-collimator are selected. In this way, clear imaging within 404-766nm spectral range is get and modulation transfer function between d-ray and g-ray imaging is all above 0.2 at the 120 line pairs.

3. Optic-Mechanical Design of Digital System Measuring Refractive Index

3.1. Collimator Design

The optical system employs transmissive optical structure. This paper makes a modification design based on the traditional structure of the telephoto lens, which achieve a good image quality to meet the aberration requirements of wave aberration, lateral color, and distortion in a wide range of wave spectrum. The parameters of collimator designed by professional ZMAX software are as follows:

Table 2. Parameters of Collimator

| Surface : type | Radius | Thickness | Glass | Semi-Diameter | Conic | |
|----------------|----------|-------------|-------|---------------|-------|-------|
| OBJ | Standard | Infinity | | Infinity | 0.000 | |
| 1 | Standard | 45.024 | V | 3.500 | K9 | 0.000 |
| 2 | Standard | -72.149 | V | 2.000 | ZF2 | 0.000 |
| 3 | Standard | -4.052E+004 | V | 43.000 | | 0.000 |
| STO | Standard | Infinity | | 61.777 | V | 0.000 |
| IMA | Standard | Infinity | | - | | 4.001 |
| | | | | | | 0.000 |

Its performance parameters, such as MTF graph, wavefront map, spherical aberration diagram, longitudinal aberration, are shown in Figure 2:

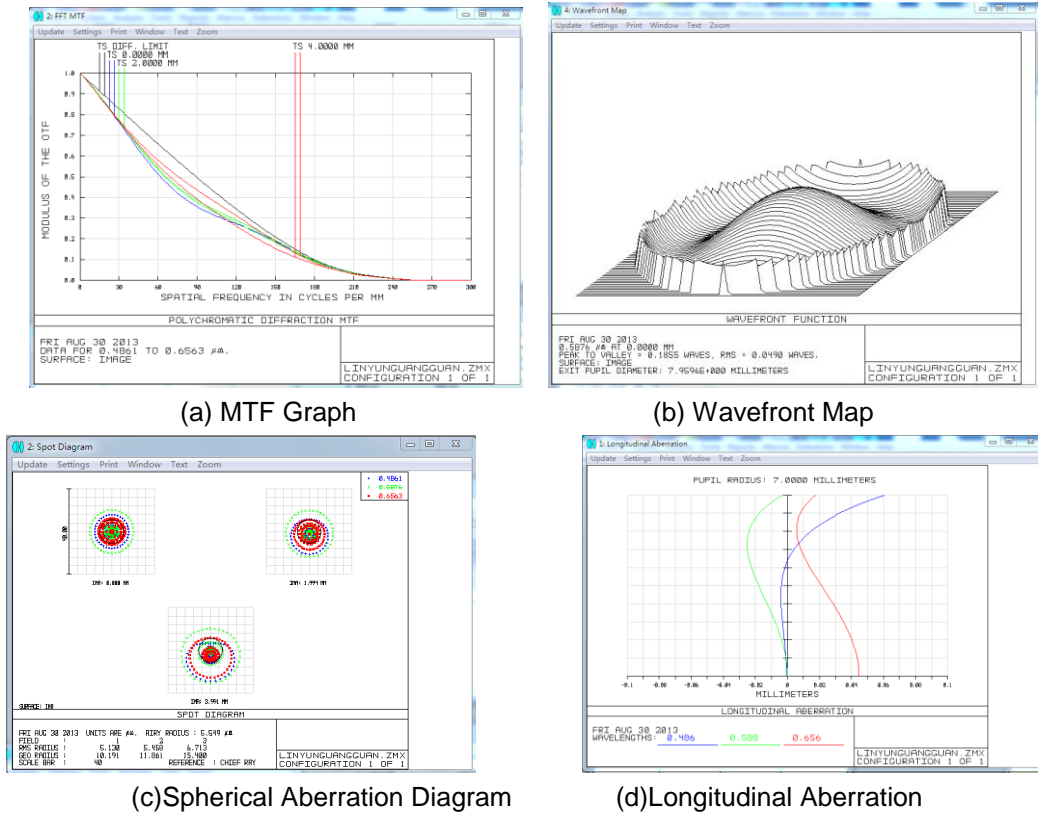
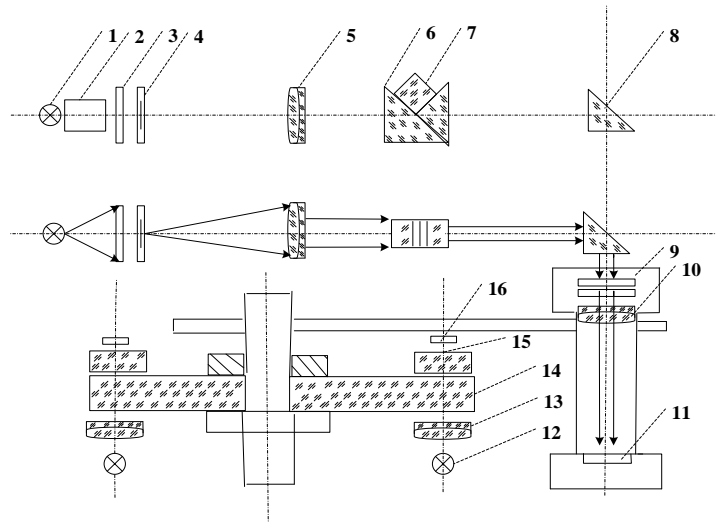


Figure 2. Collimator Performance Parameters

Rectangular prism is added into the optical system to make the system smaller, and the optical structure is shown in Figure 3.



1-source;2-monochromator;3-ground glass;4-single line reticle;5-collimator objective;6-V prism table;7-sample to be tested;8-rectangular prism;9-polaroid group;10-objective lens;11-CCD;12-light emitting diode;13-lens;14-circular grating;15-indicative grating;16-receiving device

Figure 3. Optical Structure

3.2. Mechanical Design

The structure of digital system measuring refractive index is shown in Figure 1. The CCD image of light refraction should be located in the middle of two reference lines. Taking this condition into account, the reference line is pre-set by the software. The system is designed with transmission mechanism, precision fine-tuning, and locking mechanism to achieve precise alignment of double lines clamping single one.

3.2.1. Transmission Mechanism

When clamping single line with double lines by pitching and swinging CCD, the transmission mechanism is crucial for the accuracy of refraction angle which is measured by incremental encoder. The stability of mechanical structure and the stationarity of debugging is the key. The transmission mechanism of digital system measuring refractive index is shown in Figure 4.

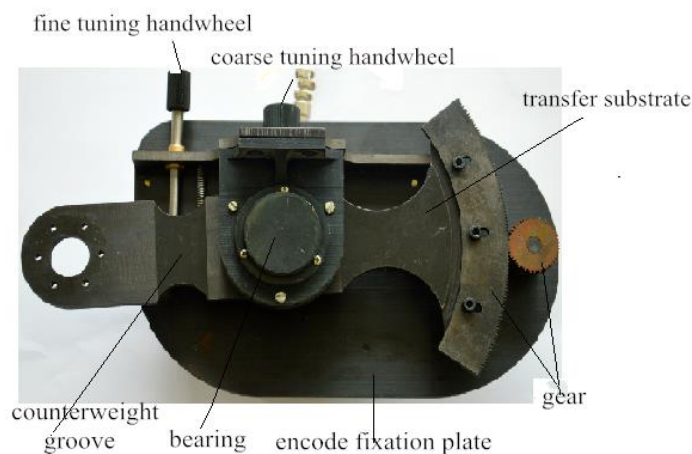


Figure 4. Transmission Mechanism

Due to the high accuracy of the encoder resolution, gradual subdivision can be achieved in gear drive used by transmission during assembling/adjusting. In order to realize the Stationary motion and meet the requirements of strength, gear modulus takes 0.5, and the transmission ratio of transmission mechanism is 476/52 for coarse tuning. The encoder output shaft is furnished with deep groove ball bearings to reduce the radial load.

3.2.2. Locking and Trimming Mechanism

In order to make the trace movement of the output shaft of the encoder slow and steady, it is adjusted to the desired precise location. The micro-motion trimming mechanism with screw transmission is used in the design of trimming mechanism. The locking mechanism is designed by the method of micro-stress clamping. The locking and trimming mechanism structure is shown in Figure 5. The output shaft of the encoder is fixed on the mounting seat by clamped ring with rubber bearing. The trimming mechanism uses one-way contact method. The screw pair is always in the role of one-way axial force using the spring to pull down clamped ring. This can guarantee unilateral contact in screw pair, and the gap does not cause empty travel. The transmission ratio of trimming mechanism K and sensitivity ΔP is given by the formula (1) and (2):

$$K = \frac{\pi D}{P} \times \frac{L}{R} \quad (1)$$

D is the diameter of the hand wheel, P is the pitch of the fretting screw and $P = 0.5mm$, R, L are shown in Figure. 6, the transmission ratio $K = 500$.

$$\Delta P = \frac{P}{2\pi} \times \frac{1}{L} \Delta \varphi \quad (2)$$

The sensitivity of human hand $\Delta \varphi$ takes 0.25° , the sensitivity ΔP is up to $0.3''$.

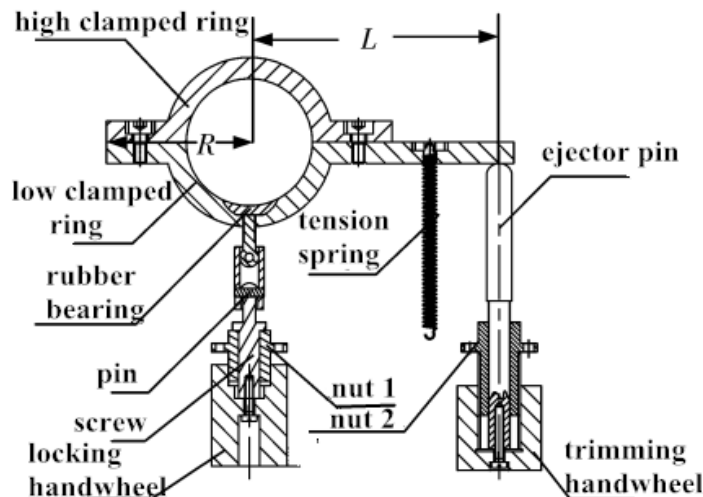


Figure 5. Locking and Trimming Mechanism

4. System Error Analysis

There are three main sources of measurement error of measuring the refractive index: the system error caused by the air refraction index; the measurement error of refraction angle; the measurement error caused by the standard deviation of refractive index n_0 .

4.1. The Error Caused by Air Refraction Index

There are many studies on precise measurements of the refractive index [4-7], but the research on the modified formula of environmental conditions is less [8, 9]. For high-precision V-prism refractometer, different testing environments such as temperature, pressure, humidity will affect the air refraction index, which causes measurement errors. Taking the influence factor of the air refraction index into account, the modified principle formula is:

$$n = \sqrt{n_0^2 + n_r \sin \theta} \sqrt{n_0^2 - n_r^2 \sin^2 \theta} \quad (3)$$

Where n is the refractive index of the sample to be tested, n_0 is the refractive index of the V-prism, θ is the deflection angle of the outgoing light relative to the incident light, n_r is the air refraction index.

The French physical scientist Adler obtained the calculation formula of the air refraction index [10]:

$$n_{t,p,f} = \frac{P \cdot (n_s - 1)}{93214 \cdot 6} \times \left[\frac{1 + P \cdot (0.5953 - 0.009876)}{1 + 0.0036610 \cdot t} \right] + 1 - f \cdot (3.802 - 0.0384 \sigma^2) \times 10^{-8} \quad (4)$$

Among them, $n_{t,p,f}$ is the air refractive index, n_s is the refractive index the sample to be tested under standard conditions, P is pressure, t is the ambient temperature, f is the environmental humidity, σ is the wave number in vacuum.

Bringing temperature, pressure and humidity into the formula, the air refractive index n_r of the C, F, d, g, e spectra are calculated under standard environmental conditions, and take partial derivative of the correction equation (3) with respect to n_r to get formula

(5). Calculating the error $\frac{\partial n}{\partial n_r} \sigma_{n_r}$ after the re-evaluation by modifying the air refractive

index, the results are shown in Table 3.

$$\frac{\partial n}{\partial n_r} = \frac{1}{2} \left(\sin \theta n_0^2 - 2 \sin^3 \theta n_r^2 \right) \cdot \left(n_0^2 + n_r \sin \theta \sqrt{n_0^2 - n_r^2 \sin^2 \theta} \cdot \sqrt{n_0^2 - n_r^2 \sin^2 \theta} \right)^{-\frac{1}{2}} \quad (5)$$

Table 3. Errors Caused by the Air Refractive Index N_r of the Spectra Under Standard Environmental Conditions

| spectrum | F | C | d | e | g |
|--|--------------------------|--------------------------|--------------------------|--------------------------|--------------------------|
| n_r | -2.7455×10^{-4} | -2.7154×10^{-4} | -2.7246×10^{-4} | -2.7317×10^{-4} | -2.7627×10^{-4} |
| $\frac{\partial n}{\partial n_r} \sigma_{n_r}$ | -2.573×10^{-5} | -2.3471×10^{-5} | -2.4105×10^{-5} | -2.4639×10^{-5} | -2.7287×10^{-5} |

From the above table, the air refractive index is approximate to the vacuum refractive index in the classic principle formula of V-prism refractometer, which causes principle error of more than 2×10^{-5} . Bringing the error caused by the air refractive index into the corrected calculation formula, the measurement results are corrected to achieve the purpose of high-accuracy measurement.

4.2. The Measurement Error of Refraction Angle

4.2.1. Precision Shafting Error

The output shaft of photoelectric rotary encoder employs semi campaign structure. The size parameters of the structure are shown in Figure 6. Because the shaft cooperation gap Δd leaves the shaft to produce angle sloshing, the maximum sloshing angel Δr of deviation of the shafting from the ideal axis is:

$$\Delta r = \frac{\Delta d}{2 \left(L_c + \frac{d_z + d_0}{2} \right)} \rho = \frac{0.002}{2 \left(52 + \frac{26 + 5}{2} \right)} \times 2 \times 10^5 = 2.95'' \quad (6)$$

Where, L_c is the distance between the spindle base and the spherical center of the steel ball, d_z is the diameter of the spindle journal, d_0 is the ball diameter, ρ is the conversion coefficient from the radian to the second and $\rho=2 \times 10^5 (")$.

The error obeys uniform distribution, so the standard deviation of Δr $\sigma_{\Delta r} = \Delta r / \sqrt{3} = 1.7''$. According CCD swing range of $\pm 30^\circ$ and the rotation angle of the encoder shafting of $\pm 6^\circ$, the standard deviation of precision shafting is: $\sigma_1 = 1.7 \text{tg} 12^\circ = 0.36''$.

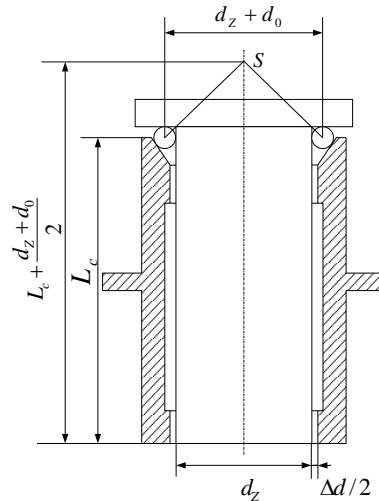


Figure 6. Schematic Diagram of Sloshing Spindle

4.2.2. CCD Interpolation Error

The pixel size is $5.2\mu\text{m}$. When the outgoing light aligns to the intermediate in two rays by screen preset, the focal length of the CCD optical system is 20mm . The interpolation error takes half pixel, and obeys uniform distribution. the CCD interpolation standard deviation σ_2 is:

$$\sigma_2 = \frac{\arctan \left(\frac{5.2 \times 10^{-3}}{2 \times 20} \right)}{\sqrt{3}} = 2.5'' \quad (7)$$

The standard deviation of refraction angle θ , σ_θ is:

$$\sigma_\theta = \sqrt{2\sigma_1^2 + \sigma_2^2 + \sigma_3^2} = 2.72'' \quad (8)$$

Where $\sigma_3=1''$ is the standard deviation of photoelectric encoder.

Taking partial derivative of the correction principle equation (3) with respect to θ , we get the measurement error caused by the standard deviation of θ .

$$\frac{\partial n}{\partial \theta} \sigma_{\theta} = \frac{1}{2} (n_r n_0^2 \cos \theta - 2 n_r^3 \cos \theta \sin^2 \theta) \cdot (n_0^2 + n_r \cos \theta \sqrt{n_0^2 - n_r^2 \sin^3 \theta} \cdot \sqrt{n_0^2 - n_r^2 \sin^2 \theta})^{-\frac{1}{2}} \cdot \sigma_{\theta} \quad (9)$$

$$= 2.82573 \times 10^{-6}$$

4.3. Measurement Error Caused by the Standard Deviation Of n_{θ} .

$\sigma_{n_{\theta}}$, the standard deviation of n_{θ} , is determined by the photoelectric precise angle measurement. The error is less than 1×10^{-6} . Taking partial derivative of the equation (3) with respect to n_{θ} , the measurement error caused by the standard deviation of n_{θ} is get.

$$\frac{\partial n}{\partial n_{\theta}} \sigma_{n_{\theta}} = \frac{1}{2} (n_0 n_r \sin \theta + 2 n_0 \sqrt{n_0^2 - n_r^2 \sin^2 \theta}) \cdot (n_0^2 \sqrt{n_0^2 - n_r^2 \sin^2 \theta} + n_r \sin \theta (n_0^2 - n_r^2 \sin^2 \theta))^{-\frac{1}{2}} \sigma_{n_{\theta}} \quad (10)$$

$$= 1.0075987 \times 10^{-6}$$

So, the measurement error of measuring the refractive index σ_n is:

$$\sigma_n = \left[\left(\frac{\partial n}{\partial n_r} \right)^2 \sigma_{n_r}^2 + \left(\frac{\partial n}{\partial n_0} \right)^2 \sigma_{n_0}^2 + \left(\frac{\partial n}{\partial \theta} \right)^2 \sigma_{\theta}^2 \right]^{\frac{1}{2}} = 3 \times 10^{-6} \quad (11)$$

The detection accuracy of refractive index is $\pm 3 \times 10^{-6}$, that is higher than the current measurement accuracy of measuring device at home and abroad.

5. Results Analysis and Conclusion

The refractive index of standard block is measured at five different spectra, which is, respectively, F, C, d, g, e light. The spectral range is 400nm-700nm. The measurement results are shown in Table 4. As can be seen from the measurement results, the measurement error is less than $\pm 3 \times 10^{-6}$.

Table 4. The Measurement Results of Refractive Index of Standard Block

| spectrum | n_0 | standard block truth-value(n) | deflection angle (θ) / '' | measurement average (n) | error/ E-6 |
|----------|-----------|-------------------------------|------------------------------------|-----------------------------|------------|
| F | 1.5159590 | 1.4923520 | -9669 | 1.4923555 | 2.0 |
| C | 1.5079303 | 1.4854211 | -9229 | 1.4854203 | -2.0 |
| d | 1.5103906 | 1.4875661 | -9348 | 1.4875501 | -1.8 |
| e | 1.5123161 | 1.4892212 | -9459 | 1.4892229 | 2.3 |
| g | 1.5202903 | 1.4960214 | -9949 | 1.4960202 | -2.4 |

In this paper, the traditional opto-mechanical structure of the system measuring refractive index has been improved. Based on the traditional structure of the telephoto lens, the auto-collimator optical system is used to meet the testing requirement of broad spectrum; trimming mechanism. The trimming mechanism with screw transmission is used in the design of trimming mechanism and the locking mechanism is designed by the method of micro-stress clamping. The incremental encoder is adopted instead of the traditional optical goniometer dial to measure the deflection angle of the outgoing light, which greatly improves the goniometer precision from original $\pm 3''$ to $\pm 1''$. Experimental results show that the measurement precision of system measuring refractive index in this paper increases to $\pm 3 \times 10^{-6}$, which is at the advanced level in the field.

References

- [1] Y. Wang, Z. Lu, H. Liu and H. Zhang, "Application of freeform surface prism", *Infrared and Laser Engineering*, vol. 3, (2007).
- [2] Y. Hori, A. Hirai and K. Minoshima, "High-accuracy interferometer with a prism pair for measurement of the absolute refractive index of glass", *Appl Opt.*, vol. 48, no. 11, (2009), pp. 2045-50.
- [3] J. W. Liu, W. Q. Liao and H. Gu, "Exploration of the Construction of Online Courses In Engineering Training Education", *Proceeding of the 9th international conference on modern industrial training*, vol. 10, (2009), pp. 202-205.
- [4] J. Li, "To Improve The Measurement Of The Brewster Angle And The Refractive Index Of The Glass By Using CCD And Spectrometer". *CDEE*, vol. 95, (2010), pp. 410-412.
- [5] X. Shang, Y. Li and X. Jiang, "Measurement of Refractive Index of Transparent Medium With Linear CCD", *Semiconductor Optoelectronics*, vol. 33, no. 3, (2012), pp. 437-440.
- [6] X. Ji and T. Chen, "Measuring Refractive Index Of Optical Glass Based On Photo-Electric Technology", *Journal of applied optics.*, vol. 31, no. 5, (2010), pp. 778-780.
- [7] G. Z. Xiao, A. Adneta and Z. Zhang, "Monitoring Changes in the Refractive index of Gases by Means of a Fiber Optic Fabry-Perot Interferometer Sensor", *Sensors and Actuators*, (2005).
- [8] J. C. Owens, "Optical refractive index of air: dependence on pressure, temperature and composition", *Applied Optics*, vol. 6 no.1, (1967), pp. 51-9.
- [9] L. Ni, Q. Ren and S. Liao, "Measurement of Cryogenic Refractive Index of IR Materials: Uncertainty Analysis", *Opto-Electronic Engineering*, vol. 37, no. 10, (2010), pp. 77-82.
- [10] F. Huang, S. Lu and S. Wang, "The Refractive Index Measurement of High Refractive Index Glass Beads[J]", *Acta Photonica Sinica*, vol. 30, no. 6, (2001), pp. 753-756.
- [11] T. Shen and X. Wei, "Effect of the Spectral Width of Optical Sources upon the Output of an Active Optical Current Sensor by Fiber Dispersion", *Journal of Harbin University of Science and Technology*, vol. 14, no. 01, (2009), pp. 98-101.

